ChemComm

ROYAL SOCIETY OF CHEMISTRY

COMMUNICATION

Cite this: *Chem. Commun.*, 2021, 57, 4015

Received 31st January 2021,
Accepted 8th March 2021

DOI: 10.1039/d1cc00484k

rsc.li/chemcomm

A novel AIE molecule as a hole transport layer enables efficient and stable perovskite solar cells†

Bin Huang,‡[ab] Yujun Cheng,‡[a] Hui Lei,‡[a] Lin Hu, *[c] Zaifang Li, [c]
Xuexiang Huang,[a] Lie Chen *[a] and Yiwang Chen [ad]

A low-cost and efficient hole transport layer (HTL) material (TPE-CZ) with the aggregation-induced emission (AIE) effect has been synthesized. Due to the AIE effect, perovskite solar cells with TPE-CZ as the HTL deliver a higher power conversion efficiency (PCE) of 18% with better stability than those with the reference HTL (Spiro-OMeTAD).

Organic–inorganic lead halide hybrid perovskite solar cells (PeSCs) have attracted great attention owing to the perovskite light absorber with exceptional intrinsic properties such as a high extinction coefficient, long electron–hole diffusion lengths, a direct band gap and high charge carrier mobilities, *etc.*[1] With the continuous effort of the scientific community, the power conversion efficiency (PCE) of PeSCs has increased from the initial 3.8% in 2009 to over 25% in 2021.[2,3] And to date, a PCE of over 24% has been achieved for commonly prepared PeSCs with regular (n-i-p type) mesoporous structures.[4]

In regular PeSCs, a compact n-type metal oxide (TiO_2, SnO_2 or ZnO) is always firstly deposited on the substrates as an electron transport layer (ETL). Then, the perovskite light absorber is deposited on top of the ETL, and subsequently coated with an organic hole transport layer (HTL) and evaporated metal as a back electrode. The organic HTL plays a critical role in efficiently extracting holes separated from the perovskite layer and simultaneously transporting them to the top metal anode.[5] Numerous organic materials have been strategically designed and synthesized to improve the performance of PeSCs in recent years. Representatives include the organic polymers poly(triaryl amine) (PTAA)[6] and poly(3-hexylthiophene) (P3HT),[7] and the small molecule 2,2′,7,7′-tetrakis(*N*,*N*-di-*p*-methoxyphenylamine)-9,9′-spirobifluorene (Spiro-OMeTAD) (Fig. 1a).[8] It is well known that batch-to-batch variation and difficulties in purification are unavoidable problems for polymers, while organic small molecules can relieve these problems and their structures are well defined. Currently, state-of-the-art PeSCs are predominantly constructed by employing the small molecule Spiro-OMeTAD as the HTL. Nevertheless, the synthesis of Spiro-OMeTAD is prohibitively expensive since it includes reaction steps that require low temperature (−78 °C) and sensitive (*n*-butyllithium or Grignard reagents) and aggressive (Br_2) reagents. Moreover, high-purity sublimation-grade Spiro-OMeTAD is required to obtain high device performance.[8] On the other hand, stability is also crucial for the commercialization of PeSCs. Extensive efforts have been made to enhance the stability *via* optimizing the morphology of the perovskite films.[3] Meanwhile, the HTL also plays an important role as a strong protective layer on the

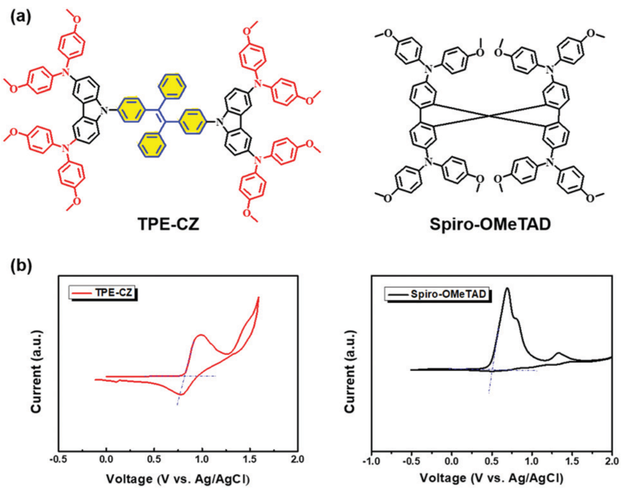

Fig. 1 (a) Molecular structures of TPE-CZ and Spiro-OMeTAD. (b) CV measurements of TPE-CZ and Spiro-OMeTAD. The ferrocene/ferrocenium (Fc/Fc^+) couple was used as an internal reference.

---

[a] *College of Chemistry/Institute of Polymers and Energy Chemistry (IPEC), Nanchang University, 999 Xuefu Avenue, Nanchang, 330031, China*
[b] *School of Metallurgical and Chemical Engineering, Jiangxi University of Science and Technology, 156 Ke Jia Road, Ganzhou, 341000, China*
[c] *China–Australia Institute for Advanced Materials and Manufacturing (IAMM), Jiaxing University, 56 Yuexiu South Avenue, Jiaxing, 314001, China*
[d] *Institute of Advanced Scientific Research (iASR), Jiangxi Normal University, 99 Ziyang Avenue, Nanchang, 330022, China*

† Electronic supplementary information (ESI) available. See DOI: 10.1039/d1cc00484k

‡ Equal contribution.

perovskites against moisture penetration and UV light to suppress the intrinsic degradation, ultimately making a contribution to the long-term stability of PeSCs. Thus, these concerns motivate a more facile and reasonable design of HTLs that can offer high efficiency with low cost production and superior stability compared to commonly used Spiro-OMeTAD.[9]

The phenomenon of aggregation-induced emission (AIE) was reported by Tang and co-workers in 2001 and is the exact opposite of the aggregation-caused quenching (ACQ) effect.[10,11] AIE molecules are generally non-fluorescent in dilute solutions because of active intramolecular motions but are induced to emit intensely in an aggregated state due to the restriction of such motions. The efficient solid-state emission of AIE molecules gives them great potential in fabricating optoelectronic devices. It has been reported that tetraphenylethylene (TPE), a classic AIE core, functioned with a methoxyphenylamine (OMe) group can serve as an efficient HTL material. Owing to the TPE-based HTL with excellent charge extraction and favorable energy alignment, these PeSCs deliver a comparable performance with those based on doped PTAA or Spiro-OMeTAD as HTLs. Although several AIE-based interlayer materials have been reported, researchers have mainly focused on improving interfacial contact, diminishing the interfacial energy barrier and facilitating charge extraction and transfer. The utilization of the unique AIE effect of these novel HTL materials to improve the device performance has rarely been examined or reported.

In this work, a novel low-cost and efficient HTL material (TPE-CZ), based on a TPE core and the *p*-methoxydiphenylamine-substituted carbazole (CZ) functional group, is developed for PeSCs (Fig. 1a). When TPE-CZ is employed as the HTL, the AIE effect of the TPE-CZ layer can convert the ultraviolet light in the incident light to visible light that is reabsorbed by the perovskite layer, leading to an improvement in the photocurrent. This AIE effect also reduces the instability of the device caused by the ultraviolet light in the incident light. Therefore, PeSCs based on TPE-CZ as the HTL achieve a higher PCE (PCE = 18.0%) than the reference devices based on the Spiro-OMeTAD HTL (PCE = 16.7%) and maintain a superior stability.

For the new HTL material, we select TPE as the core and CZ equipped with OMe as the functional group. To ensure that the resulting compound possess a good AIE effect, two CZ functional groups flank both sides of the TPE core. The target TPE-CZ molecule is synthesized in only three steps *via* the Buchwald–Hartwig cross coupling reaction. The corresponding synthetic route is shown in Scheme 1 in the ESI.† The nuclear magnetic resonance (NMR) spectra and time of flight mass spectrometry (MALDI-TOF-MS) results (with an isotopic cluster peaking at a *m*/*z* of 1570.24, calculated for M^+) synergistically confirmed the structure of TPE-CZ (Fig. S1, ESI†). Roughly calculating the cost of TPE-CZ, it is obvious that its cost is much lower than that of the commonly used Spiro-OMeTAD[9] (Table S1 and Fig. S2, ESI†). Because of the special twisted structure, TPE-CZ can easily dissolve in common organic solvents such as chloroform, chlorobenzene, toluene, *etc.* Thermo gravimetric analysis (TGA) measurements reveal that the TPE-CZ film shows good thermal stability. The TPE-CZ film starts to decompose at a temperature of around 370 °C (Fig. S3, ESI†).

To investigate the potential application of TPE-CZ as a HTL material in PeSCs, density functional theory calculations at the B3LYP/6-31G(d,p) level are applied to give insights into its highest occupied molecular orbital (HOMO) and lowest unoccupied molecular orbital (LUMO) energy levels (Fig. S4, ESI†). From the optimized molecular geometries, the HOMO mainly locates on the flanking carbazole-based triphenylamine functional group, while the LUMO spreads over part of the central TPE core. The calculated energy level is −4.26 eV for the HOMO and −1.52 eV for the LUMO. The energy levels are also determined through cyclic voltammetry (CV) measurements. As shown in Fig. 1b and Table 1, the HOMO energy level of TPE-CZ (−5.52 eV) is higher than that of Spiro-OMeTAD (−5.22 eV). The ferrocene/ferrocenium (Fc/Fc^+) couple was used as an internal reference.

The optical properties of organic semiconductors have been proved to be closely related to their aggregation behaviour, especially for this novel molecule with a twisted structure. The normalized ultraviolet-visible (UV-Vis) absorption spectrum of the TPE-CZ film is shown in Fig. 2a. The absorption band locating in the region of 300–400 nm is assigned to a high-energy π–π^* transition of the conjugated system in the molecule. When the film is excited by a light with an excitation wavelength of 352 nm, it delivers a strong fluorescence. The fluorescence locates in the region around 450–700 nm with a peak at 510 nm. The phenomenon is shown directly in Fig. 2b, where the film emits a strong white light when exposed to an ultraviolet lamp. To further explore the origins, a series of photoluminescence (PL) measurements are performed. The TPE-CZ is firstly dissolved in THF at a concentration of 3×10^{-5} M. As shown in Fig. 2c, the pristine TPE-CZ THF solution is not fluorescent when exposed to an ultraviolet lamp. However, when deionized water is added into the TPE-CZ solution to form THF/H_2O mixtures, the samples could fluoresce. Moreover, the fluorescence intensities are gradually enhanced with the increase of the water fraction (f_w) in the resultant THF/H_2O mixture. Here, water is poor solvent for the TPE-CZ molecule. The TPE-based twisted structure tends to aggregate and emission is induced when poor solvents are added into the solution. This phenomenon indicates that TPE-CZ is a typical AIE molecule. The corresponding PL spectra of the solutions are shown in Fig. 2d.

TPE-CZ is then employed as the HTL in the PeSCs. The device structure is FTO/compact TiO_2/mesoporous TiO_2/$CH_3NH_3PbI_3$/HTL/Ag (Fig. 3a). A compact and mesoporous layer of TiO_2 is deposited on top of FTO for electron collection. The organic HTL (TPE-CZ or Spiro-OMeTAD) is successively deposited on top of

Table 1 Summary of the electrochemical and physical properties of TPE-CZ and Spiro-OMeTAD

HTLs	E_{ox}[a]	E_{HOMO}[b] (eV)	Hole mobility[c] ($cm^2\ V^{-1}\ s^{-1}$)
TPE-CZ	0.81	−5.52	8.57×10^{-5}
Spiro-OMeTAD	0.51	−5.22	5.39×10^{-5}

[a] E_{ox} obtained from the cyclic voltammograms. [b] The ferrocene/ferrocenium (Fc/Fc^+) couple was used as an internal reference and its vacuum level was set to 4.71 eV. [c] Determined by the space-charge-limited current (SCLC) method.

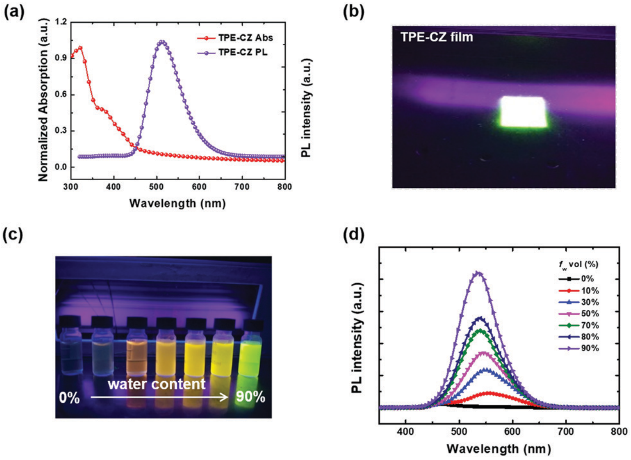

Fig. 2 (a) UV-Vis absorption spectrum and PL emission spectrum of TPE-CZ on quartz substrates. (b) Pictures of the TPE-CZ film exposed to an ultraviolet lamp. (c) The TPE-CZ THF solution (3×10^{-5} M) with various water contents exposed to an ultraviolet lamp and (d) PL spectra of the corresponding TPE-CZ solutions.

the perovskite layer, followed by a layer of evaporated Ag. The $CH_3NH_3PbI_3$ perovskite serves as the light absorber. The detailed device fabrications are described in the ESI.† A high-resolution scanning electron microscopy (SEM) cross-section image of the prepared PeSCs is shown in Fig. 3b. PeSCs with the commonly used Spiro-OMeTAD are prepared for comparison. As shown in Fig. 3c and Table 2, the optimized PeSC based on TPE-CZ as the HTL yields a high PCE of 18.0%, an open-circuit voltage (V_{OC}) of 1.08 V, a short-circuit current density (J_{SC}) of 21.47 mA cm^{-2}and a fill factor (FF) of 77.5%. The hysteresis effect of the PeSCs is negligible when the device is scanned in the reverse and forward directions. *J–V* characteristics of the PeSCs based on TPE-CZ with various mass concentrations are shown in Fig. S5 (ESI†). The detailed device performance is summarized in Table S2 (ESI†). The optimized device performance is superior to that of the PeSCs based on Spiro-OMeTAD as the HTL with a PCE of 16.7%, a V_{OC} of 1.09 V, a J_{SC} of 20.17 mA cm^{-2}and a FF of 75.9%. After applying a bias at the maximum output voltage, a more stable power output is also obtained (Fig. S6, ESI†). It is obvious that the improvement of the device's performance is mainly owed to the enhanced J_{SC} and FF, indicating the more efficient hole extraction and collection from the TPE-CZ HTL to the top electrode. The external quantum efficiency (EQE) spectra are consistent with the results from the *J–V* characteristics (Fig. 3c). Interestingly, we note that an additional spectrum response in the near ultraviolet region is found for the PeSCs based on TPE-CZ as the HTL. Combined with the aforementioned novel optical properties (Fig. 2), this can be presumably attributed to TPE-CZ absorbing the incident ultraviolet light and emitting fluorescence that can be absorbed again by the perovskite layer. This point is in agreement with the phenomenon that the sample of FTO/compact TiO_2/mesoporous TiO_2/$CH_3NH_3PbI_3$ possesses a lower transmittance in the near ultraviolet region after coating with a TPE-CZ layer (Fig. S7, ESI†). Therefore, the enhanced J_{SC} confirms the positive effect caused by the TPE-CZ HTL with the novel AIE characteristic.

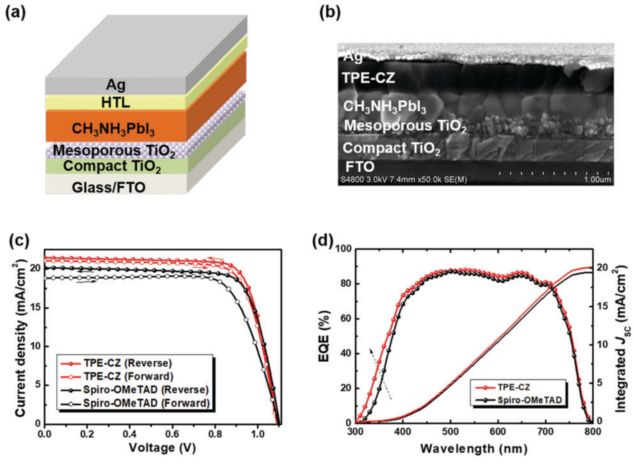

Fig. 3 (a) Schematic of the device structure. (b) SEM cross-section image of the prepared PeSCs. (c) *J–V* characteristics of the optimized PeSCs based on TPE-CZ as the HTL. The device-based on Spiro-OMeTAD as the HTL is used for comparison. (d) The corresponding EQE spectra for the PeSCs.

To further investigate the improvement of the device performance, steady state PL and time-resolved PL (TRPL) measurements are employed to evaluate the hole extraction in the PeSCs (as seen in Fig. 4a). The pristine $CH_3NH_3PbI_3$ film possesses a strong photoluminescence centered at 760 nm. The PL spectrum is obviously quenched after depositing a HTL on top of the perovskite film. Moreover, the PL quenching is more pronounced for $CH_3NH_3PbI_3$/TPE-CZ than for $CH_3NH_3PbI_3$/Spiro-OMeTAD, suggesting the more efficient hole extraction from $CH_3NH_3PbI_3$ to TPE-CZ. The result agrees with the point that TPE-CZ possesses a better matched energy alignment with the perovskite layer for hole extraction. The corresponding TRPL decay of the samples is shown in Fig. 4b. A bi-exponential decay model is used to fit the PL decay curves to obtain an average exciton lifetime (τ_{ave}) (Table S3, ESI†). The pristine $CH_3NH_3PbI_3$ layer presents a τ_{ave} of 26.1 ns. After depositing a Spiro-OMeTAD HTL on top of the $CH_3NH_3PbI_3$ layer, the exciton lifetime decays rapidly and the τ_{ave} decreases to 4.7 ns. When TPE-CZ serves as the HTL, the τ_{ave} decreases more significantly to 3.3 ns, indicating more efficient charge transfer. The better charge transfer between the perovskite layer and the TPE-CZ layer plays a considerable role in improving the device performance. In addition, the carrier mobility is determined by the space-charge limited currents (SCLCs) to elucidate the charge transportation in the devices. The structure of the hole-only devices is ITO/PEDOT:PSS/$CH_3NH_3PbI_3$/TPE-CZ or Spiro-OMeTAD/Ag. Fig. S8 (ESI†) shows their *J–V* characteristics measured in the dark. According to the Mott–Gurney equation, the obtained hole mobility of TPE-CZ is 8.57×10^{-5} cm^2 V^{-1} s^{-1}, which is higher than that of Spiro-OMeTAD (5.39×10^{-5} cm^2 V^{-1} s^{-1}). The improved hole mobility would reduce the carrier's loss when they are transported through the interlayer. The PeSCs based on the TPE-CZ HTL thus obtain a superior device performance, especially maintaining a high FF.

The stability of a device is an issue of increasing concern for the scientific community. It is well known that the decomposition

Table 2 The device parameters based on TPE-CZ and Spiro-OMeTAD as the HTLs

HTLs	J_{SC} (mA cm^{-2})	V_{OC} (V)	FF (%)	PCE$_{max}$/PCE$_{ave}$^{a} (%)
TPE-CZ (reverse)	21.47 ± 0.3	1.08 ± 0.01	77.5 ± 1.0	18.0/17.8 ± 0.20
TPE-CZ (forward)	21.07 ± 0.3	1.08 ± 0.01	75.7 ± 1.0	17.2/16.9 ± 0.3
Spiro-OMeTAD (reverse)	20.17 ± 0.1	1.09 ± 0.01	75.9 ± 0.6	16.7/16.5 ± 0.3
Spiro-OMeTAD (forward)	18.81 ± 0.2	1.09 ± 0.01	73.8 ± 0.4	15.1/15.0 ± 0.1

[a] Average PCE values are calculated from ten individual cells.

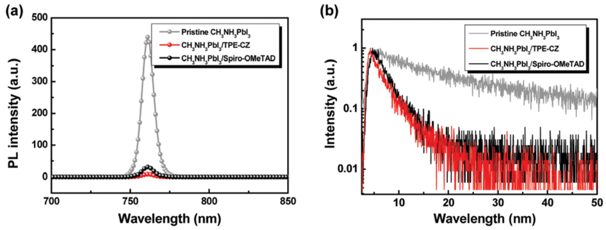

Fig. 4 (a) The steady state PL spectra and (b) TRPL spectra of pristine $CH_3NH_3PbI_3$, $CH_3NH_3PbI_3$/TPE-CZ and $CH_3NH_3PbI_3$/Spiro-OMeTAD.

of perovskite crystals usually occurs, and that the devices degrade faster when exposed to UV light, moisture, oxygen, *etc.* We firstly investigated the UV light stability of the devices. The devices were stored in a N_2-filled glove box under UV light illumination (365 nm, 8 W) without encapsulation. As shown in Fig. S9a (ESI†), the device based on TPE-CZ as the HTL maintains ∼60% of its initial PCE after 6 h of UV light irradiation, while the reference device based on the Spiro-OMeTAD HTL only delivers ∼30% under the same exposure conditions. The enhanced UV stability presumably originates from the TPE-CZ molecule with a novel optical property. During the test of the UV light stability, the ultraviolet light is incident from the FTO side into the device while it will be reflected by the top opaque Ag electrode. When the reflected ultraviolet light passes through the HTL, the TPE-CZ molecules will absorb the ultraviolet light and convert it into visible light, thereby reducing the damage to the perovskite layer. The humidity and air stability of the PeSCs are also measured. The PeSCs without encapsulation were stored in a Petri dish in ambient conditions (25 °C, humidity ∼50%). To reduce the impact caused by the indoor light, the Petri dish was wrapped with opaque tin foil. As shown in Fig. S9b (ESI†), the reference PeSC exhibits extremely inferior stability. Its PCE drops to less than 20% after being stored in ambient conditions for 10 days. The decline of the PCE is presumably attributed to the damage caused by the penetration of moisture or oxygen into the functional layers, especially for the perovskite layer. However, the TPE-CZ layer is more hydrophobic (Fig. S10, ESI†). It can prevent the penetration of moisture and oxygen into the device which would cause a detrimental effect. Thus, the PeSC possesses a much enhanced stability in ambient conditions with 63% of its initial PCE.

In summary, the twisted AIE molecule TPE-CZ has been designed and synthesized by a facile straightforward synthetic route. TPE-CZ can be employed as an efficient HTL to improve the PCE and stability of PeSCs. Careful investigations demonstrate that TPE-CZ can convert the ultraviolet light in the incident light into visible light. The visible light is absorbed by the perovskite to improve the photocurrent. Moreover, this AIE characteristic eliminates the notorious detrimental effect to the device stability caused by the ultraviolet light. Therefore, an excellent PCE of 18% and much better stability are achieved for the PeSCs based on TPE-CZ as the HTL, which is higher than the reference PeSCs based on Spiro-OMeTAD as the HTL (PCE = 16.7%). This work provides a new route to develop PeSCs with high efficiency as well as long-term stability.

Conflicts of interest

There are no conflicts to declare.

Notes and references

1 M. Liu, M. B. Johnston and H. J. Snaith, *Nature*, 2013, **501**, 395–398.
2 A. Kojima, K. Teshima, Y. Shirai and T. Miyasaka, *J. Am. Chem. Soc.*, 2009, **131**, 6050–6051.
3 National Renewable Energy Laboratory, Best research-cell efficiencies chart, 2020, www.nrel.gov/pv/assets/pdfs/bestresearch-cell-efficiencies, 20200218.pdf.
4 M. Kim, G.-H. Kim, T. K. Lee, I. W. Choi, H. W. Choi, Y. Jo, Y. J. Yoon, J. W. Kim, J. Lee and D. Huh, *Joule*, 2019, **3**, 2179–2192.
5 H. Chen, W. Fu, C. Huang, Z. Zhang, S. Li, F. Ding, M. Shi, C. Z. Li, A. K. Y. Jen and H. Chen, *Adv. Energy Mater.*, 2017, **7**, 1700012.
6 N. J. Jeon, J. H. Noh, W. S. Yang, Y. C. Kim, S. Ryu, J. Seo and S. I. Seok, *Nature*, 2015, **517**, 476–480.
7 H. Lu, Y. Ma, B. Gu, W. Tian and L. Li, *J. Mater. Chem. A*, 2015, **3**, 16445–16452.
8 M. Saliba, S. Orlandi, T. Matsui, S. Aghazada, M. Cavazzini, J.-P. Correa-Baena, P. Gao, R. Scopelliti, E. Mosconi, K.-H. Dahmen, F. De Angelis, A. Abate, A. Hagfeldt, G. Pozzi, M. Graetzel and M. K. Nazeeruddin, *Nat. Energy*, 2016, **1**, 15017.
9 Y. Li, K. R. Scheel, R. G. Clevenger, W. Shou, H. Pan, K. V. Kilway and Z. Peng, *Adv. Energy Mater.*, 2018, **8**, 1801248.
10 J. Luo, Z. Xie, J. W. Y. Lam, L. Cheng, B. Z. Tang, H. Chen, C. Qiu, H. S. Kwok, X. Zhan and Y. Liu, *Chem. Commun.*, 2001, 1740–1741.
11 Y. Chen, J. W. Y. Lam, R. T. K. Kwok, B. Liu and B. Z. Tang, *Mater. Horiz.*, 2019, **6**, 428–433.